Jet Formation in the Equatorial Oceans Through Barotropic and Inertial Instabilities

Mark Fruman

Bach Lien Hua, Richard Schopp,
Marc d'Orgeville, Claire Ménesguen

LPO – IFREMER, Brest, France

IAU Seminar, 22.10.2008

Johann Wolfgang Goethe Universität-Frankfurt

Jet Formation in the Equatorial Oceans Through Barotropic and Inertial Instabilities

- equatorial jets in the ocean (motivation)

Jet Formation in the Equatorial Oceans Through Barotropic and Inertial Instabilities

- equatorial jets in the ocean (motivation)
- barotropic instability of equatorial waves

Jet Formation in the Equatorial Oceans Through Barotropic and Inertial Instabilities

- equatorial jets in the ocean (motivation)
- barotropic instability of equatorial waves
- the role of inertial instability in jet formation

Jet Formation in the Equatorial Oceans Through Barotropic and Inertial Instabilities

- equatorial jets in the ocean (motivation)
- barotropic instability of equatorial waves
- the role of inertial instability in jet formation
- applications

Motivation

- Observations of the equatorial Atlantic:

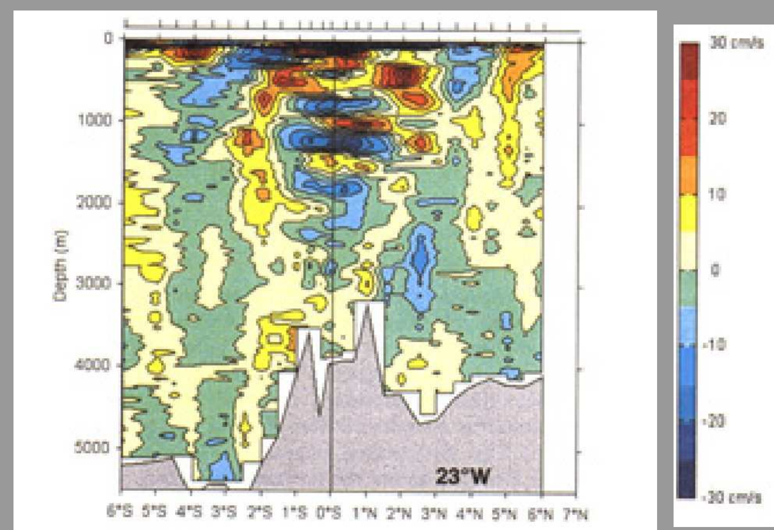

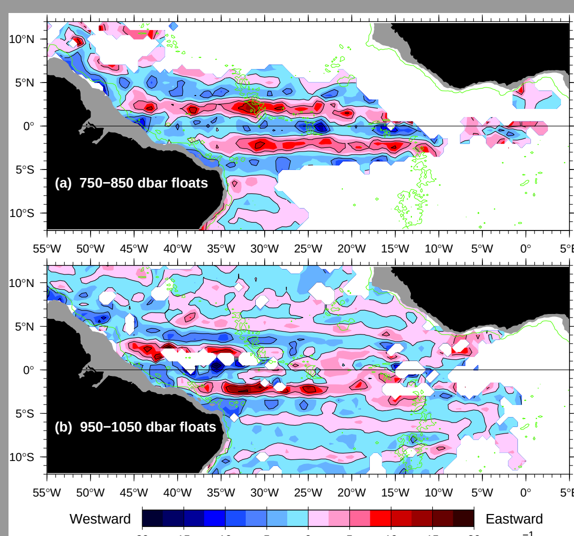

Motivation

- Observations of the equatorial Atlantic:

Gouriou et al. 2001 $\Longrightarrow$

– instantaneous merid. sect. 23° W

– strongly barotropic jets

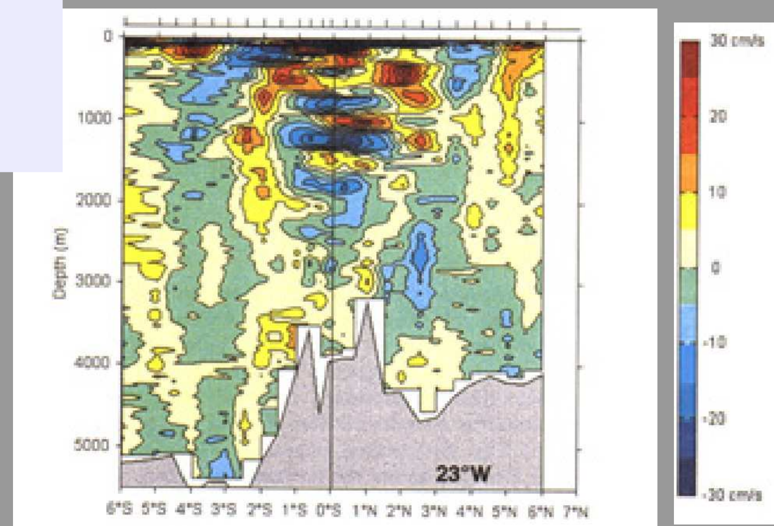

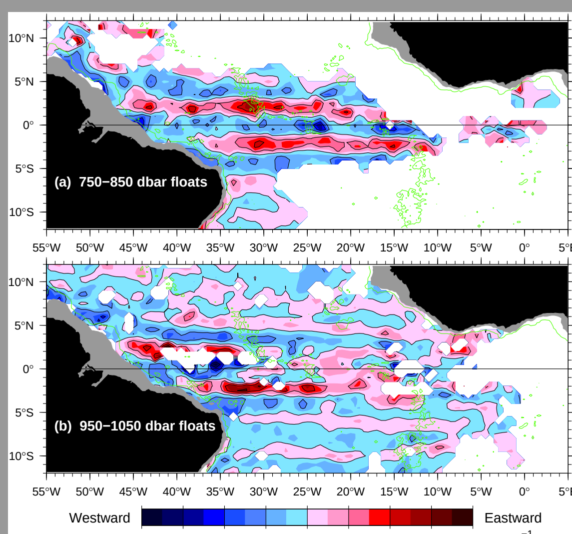

Motivation

- Observations of the equatorial Atlantic:

Gouriou et al. 2001 $\Longrightarrow$

– instantaneous merid. sect. 23° W

– strongly barotropic jets

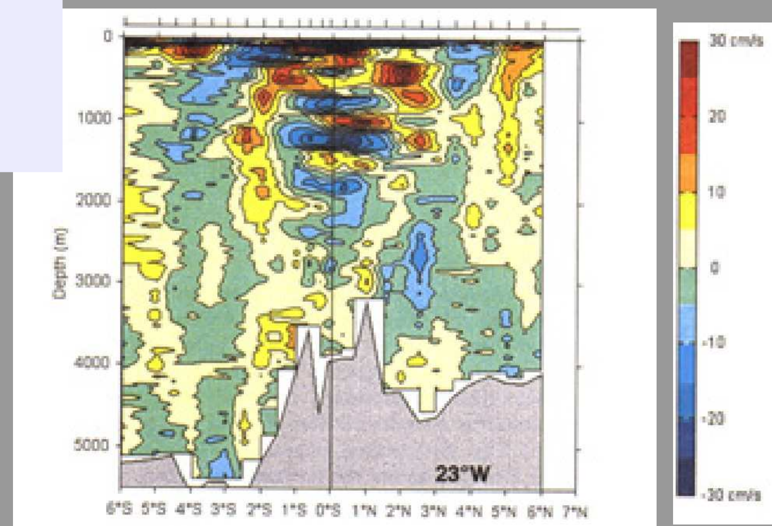

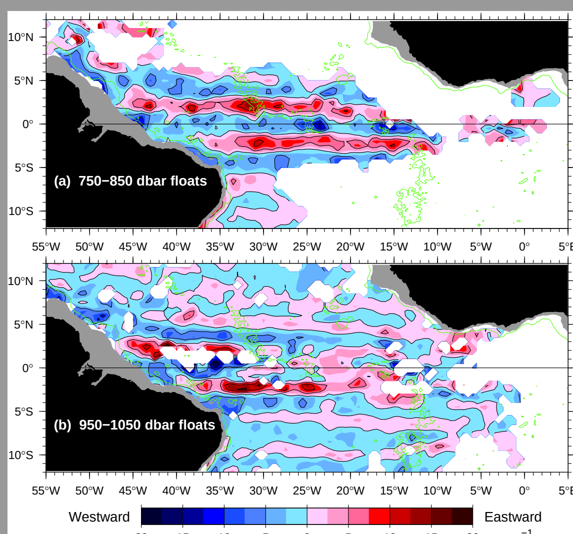

$\Longleftarrow$ Ollitrault et al. 2006

– zonal currents near 1000 m depth

– multiple, equally spaced jets

Motivation

- Observations of the equatorial Atlantic:

Motivation

- Observations of the equatorial Atlantic:
  - low-frequency variability (30-60 days) in meridional velocity, predominantly near western boundary and coherent over $\mathcal{O}(1000\text{m})$ depth (Bunge et al., 2006)

Motivation

- Observations of the equatorial Atlantic:
  - low-frequency variability (30-60 days) in meridional velocity, predominantly near western boundary and coherent over $\mathcal{O}$(1000m) depth (Bunge et al., 2006)
  - zonally symmetric zonal velocity with strong barotropic component (Gouriou et al., 2001)

Motivation

- Observations of the equatorial Atlantic:
  - low-frequency variability (30-60 days) in meridional velocity, predominantly near western boundary and coherent over $\mathcal{O}$(1000m) depth (Bunge et al., 2006)
  - zonally symmetric zonal velocity with strong barotropic component (Gouriou et al., 2001)
  - symmetry about the equator in both zonal and meridional velocity (Bourles et al., 2003).

Motivation

- Observations of the equatorial Atlantic:
  - low-frequency variability (30-60 days) in meridional velocity, predominantly near western boundary and coherent over $\mathcal{O}(1000\text{m})$ depth (Bunge et al., 2006)
  - zonally symmetric zonal velocity with strong barotropic component (Gouriou et al., 2001)
  - symmetry about the equator in both zonal and meridional velocity (Bourles et al., 2003).

- Dispersion diagram for meridionally confined equatorial waves:

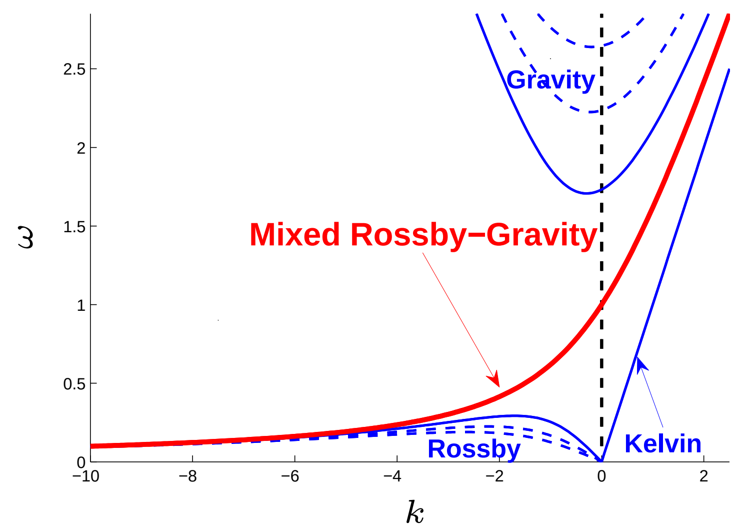

Motivation

- Observations of the equatorial Atlantic:
  - low-frequency variability (30-60 days) in meridional velocity, predominantly near western boundary and coherent over $\mathcal{O}$(1000m) depth (Bunge et al., 2006)
  - zonally symmetric zonal velocity with strong barotropic component (Gouriou et al., 2001)
  - symmetry about the equator in both zonal and meridional velocity (Bourles et al., 2003).

- Dispersion diagram for meridionally confined equatorial waves:
  - Short wavelength Rossby and mixed Rossby-gravity waves have low-frequency and eastward group velocity.
  - Variability near western boundary could excite such waves which would then propagate into the interior.

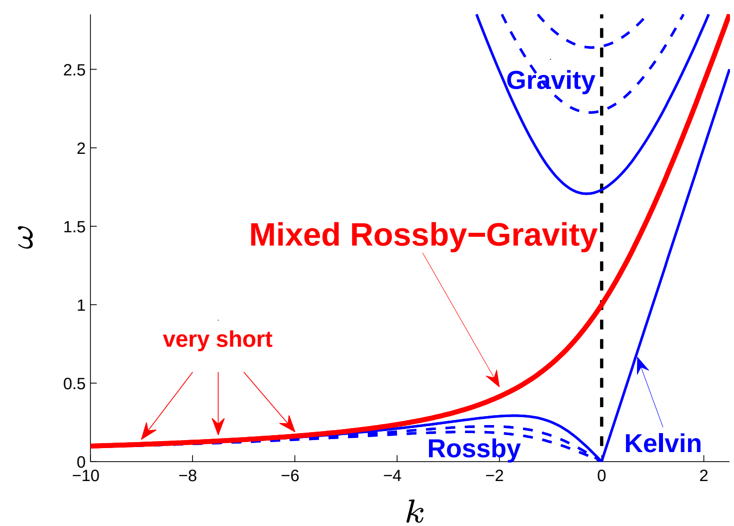

Jet formation through wave instability

- In the short wavelength limit, the instability of barotropic Rossby waves (Lorenz, 1972; Gill, 1974; Lee and Smith, 2003) leads to the formation of zonal jets (Manfroi and Young, 1999).

Jet formation through wave instability

- In the short wavelength limit, the instability of barotropic Rossby waves (Lorenz, 1972; Gill, 1974; Lee and Smith, 2003) leads to the formation of zonal jets (Manfroi and Young, 1999).
- Equatorial Rossby and mixed Rossby-gravity (MRG) waves have dispersion relations and velocity fields similar to barotropic Rossby waves and are thus subject to the same barotropic instability (even though they are inherently baroclinic).

Jet formation through wave instability

- In the short wavelength limit, the instability of barotropic Rossby waves (Lorenz, 1972; Gill, 1974; Lee and Smith, 2003) leads to the formation of zonal jets (Manfroi and Young, 1999).
- Equatorial Rossby and mixed Rossby-gravity (MRG) waves have dispersion relations and velocity fields similar to barotropic Rossby waves and are thus subject to the same barotropic instability (even though they are inherently baroclinic).

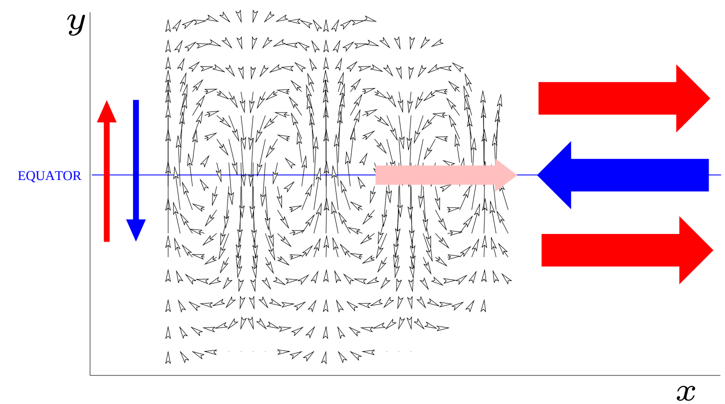

- Numerical simulations of MRG waves excited from the western boundary show that they can lead to zonal jets:
  - Baroclinic equatorial deep jets (d'Orgeville et al., 2007; Hua et al., 2008)
  - Extra-equatorial barotropic jets (Ménesguen et al., submitted)

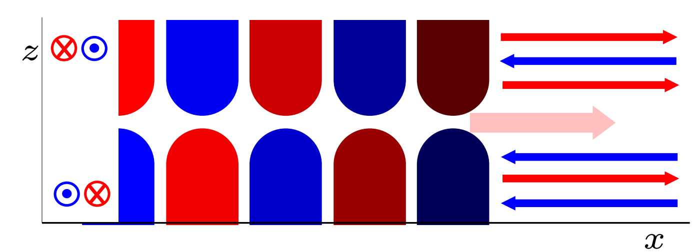

Simulations of low frequency MRG waves

- To understand the basic mechanism performed high-resolution Primitive Equations simulations using the Regional Ocean Modeling System (ROMS) (Shchepetkin and McWilliams, 2005) initialized with a mixed Rossby-gravity wave in a zonally-periodic reentrant β-plane channel.

Simulations of low frequency MRG waves

- To understand the basic mechanism performed high-resolution Primitive Equations simulations using the Regional Ocean Modeling System (ROMS) (Shchepetkin and McWilliams, 2005) initialized with a mixed Rossby-gravity wave in a zonally-periodic reentrant β-plane channel.
- Fixed parameters were:
  - buoyancy frequency $N = 2 \times 10^{-3}$ s^{-1}
  - ocean depth $H = 5000$ m
  - vertical mode 1, with wavelength 10000 m

Simulations of low frequency MRG waves

- To understand the basic mechanism performed high-resolution Primitive Equations simulations using the Regional Ocean Modeling System (ROMS) (Shchepetkin and McWilliams, 2005) initialized with a mixed Rossby-gravity wave in a zonally-periodic reentrant β-plane channel.
- Fixed parameters were:
  - buoyancy frequency $N = 2 \times 10^{-3}$ s^{-1}
  - ocean depth $H = 5000$ m
  - vertical mode 1, with wavelength 10000 m
- giving:
  - a gravest mode Kelvin wave speed $c \equiv \frac{NH}{\pi} = 3.2$ m s^{-1}
  - an equatorial deformation radius $L_D \equiv \sqrt{\frac{c}{\beta}} = 375$ km

Simulations of low frequency MRG waves

- To understand the basic mechanism performed high-resolution Primitive Equations simulations using the Regional Ocean Modeling System (ROMS) (Shchepetkin and McWilliams, 2005) initialized with a mixed Rossby-gravity wave in a zonally-periodic reentrant β-plane channel.
- Fixed parameters were:
  - buoyancy frequency $N = 2 \times 10^{-3}$ s^{-1}
  - ocean depth $H = 5000$ m
  - vertical mode 1, with wavelength 10000 m
- giving:
  - a gravest mode Kelvin wave speed $c \equiv \frac{NH}{\pi} = 3.2$ m s^{-1}
  - an equatorial deformation radius $L_D \equiv \sqrt{\frac{c}{\beta}} = 375$ km
- Parameters varied were the amplitude of meridional velocity V_0^* and the zonal wavelength λ_x, or in nondimensional terms:
  - Froude number $V_0 \equiv \dfrac{V_0^*}{c}$, zonal wavenumber $k = 2\pi \dfrac{L_D}{\lambda_x}$

Simulations of low frequency MRG waves

- Considered cases with $-6 < k < -16$ (wavelengths between 150 km and 350 km)

Simulations of low frequency MRG waves

- Considered cases with $-6 < k < -16$ (wavelengths between 150 km and 350 km)
- Dispersion relation:

$$\omega \equiv \frac{\omega^*}{\sqrt{\beta c}} = \frac{1}{2}\left(k + \sqrt{k^2 - 4}\right)$$

- For vertical mode 1, simulations have wave periods between 50 and 200 days.

Simulations of low frequency MRG waves

- Considered cases with $-6 < k < -16$ (wavelengths between 150 km and 350 km)
- Dispersion relation:

$$\omega \equiv \frac{\omega^*}{\sqrt{\beta c}} = \frac{1}{2}\left(k + \sqrt{k^2 - 4}\right)$$

- For vertical mode 1, simulations have wave periods between 50 and 200 days.
- In the $k \ll -1$ (low frequency) limit,

$$\omega \sim -\frac{1}{k}$$

Simulations of low frequency MRG waves

- Considered cases with $-6 < k < -16$ (wavelengths between 150 km and 350 km)
- Dispersion relation:

$$\omega \equiv \frac{\omega^*}{\sqrt{\beta c}} = \frac{1}{2}\left(k + \sqrt{k^2 - 4}\right)$$

- For vertical mode 1, simulations have wave periods between 50 and 200 days.
- In the $k \ll -1$ (low frequency) limit,

$$\omega \sim -\frac{1}{k}$$

$\Longrightarrow$ zonal shear in meridional velocity dominates the β effect (rotation) and ω (wave propagation).

Simulations of low frequency MRG waves

- Simulation with $V_0 = 0.11$ (0.36 cm amplitude) and $k = -6.3$ (350 km wavelength)
  - at $0.1^\circ \times 0.1^\circ$ horizontal resolution ($1^\circ \approx 100$km)
  - 100-200 vertical levels (25-50 m vertical resolution)

Simulations of low frequency MRG waves

- Simulation with $V_0 = 0.11$ (0.36 cm amplitude) and $k = -6.3$ (350 km wavelength)
  - at $0.1^\circ \times 0.1^\circ$ horizontal resolution ($1^\circ \approx 100$km)
  - 100-200 vertical levels (25-50 m vertical resolution)

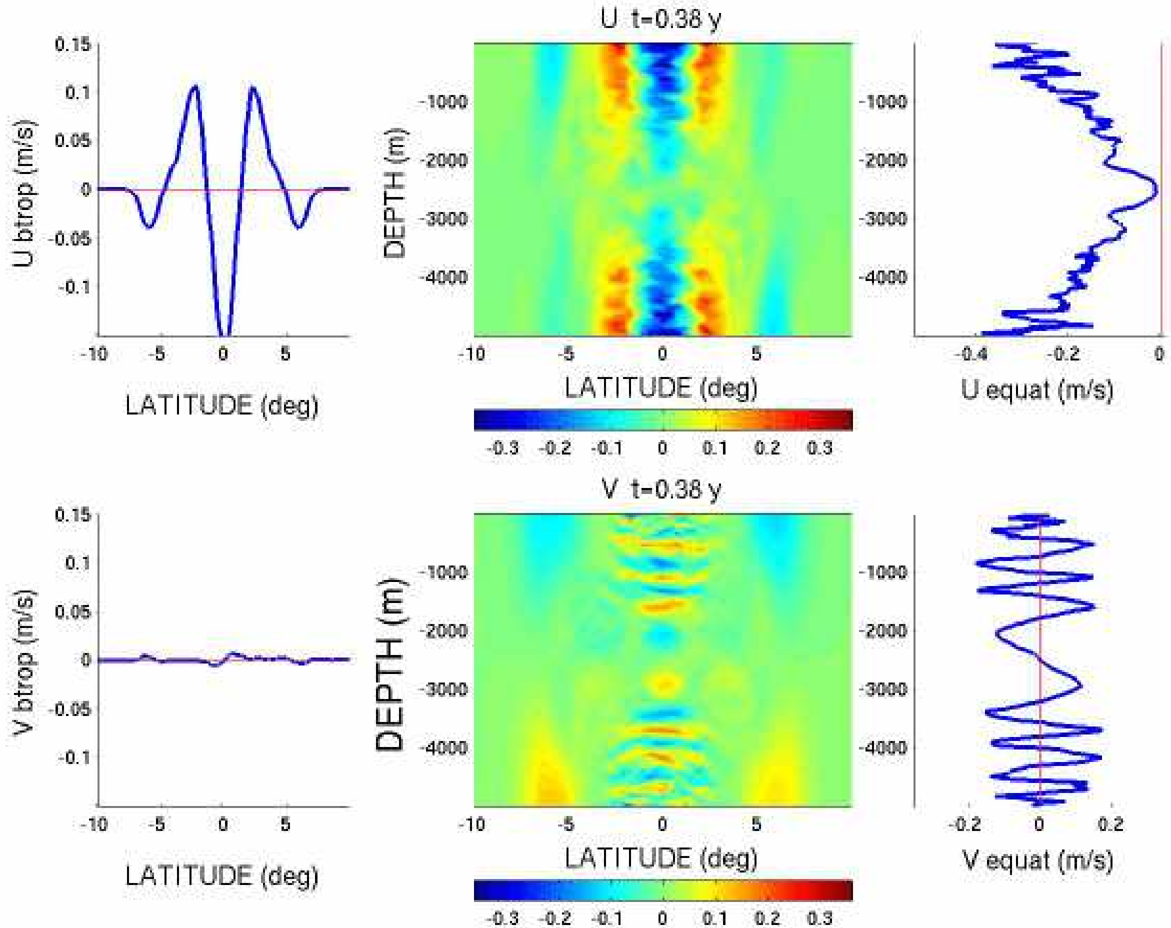

Simulations of low frequency MRG waves

- Simulation with $V_0 = 0.11$ (0.36 cm amplitude) and $k = -6.3$ (350 km wavelength)
  - at $0.1° \times 0.1°$ horizontal resolution ($1° \approx 100$km)
  - 100-200 vertical levels (25-50 m vertical resolution)

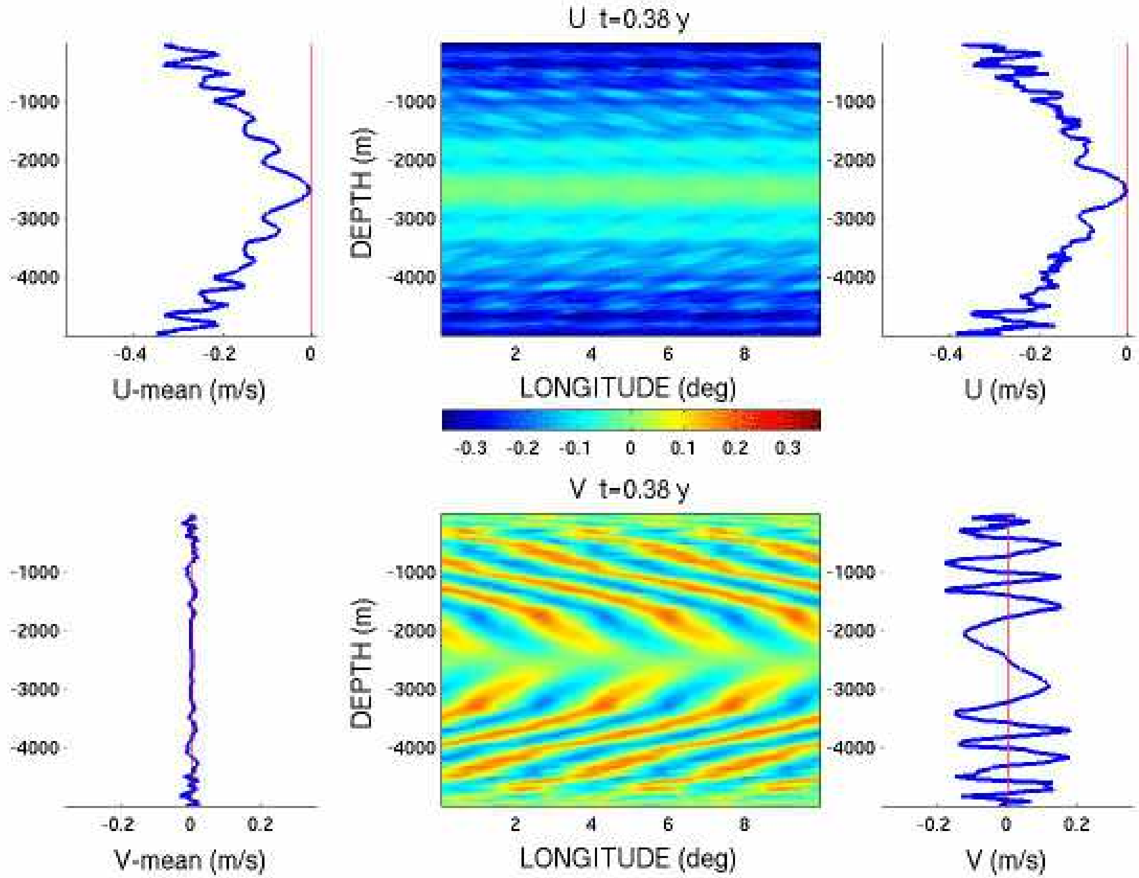

Barotropic Instability

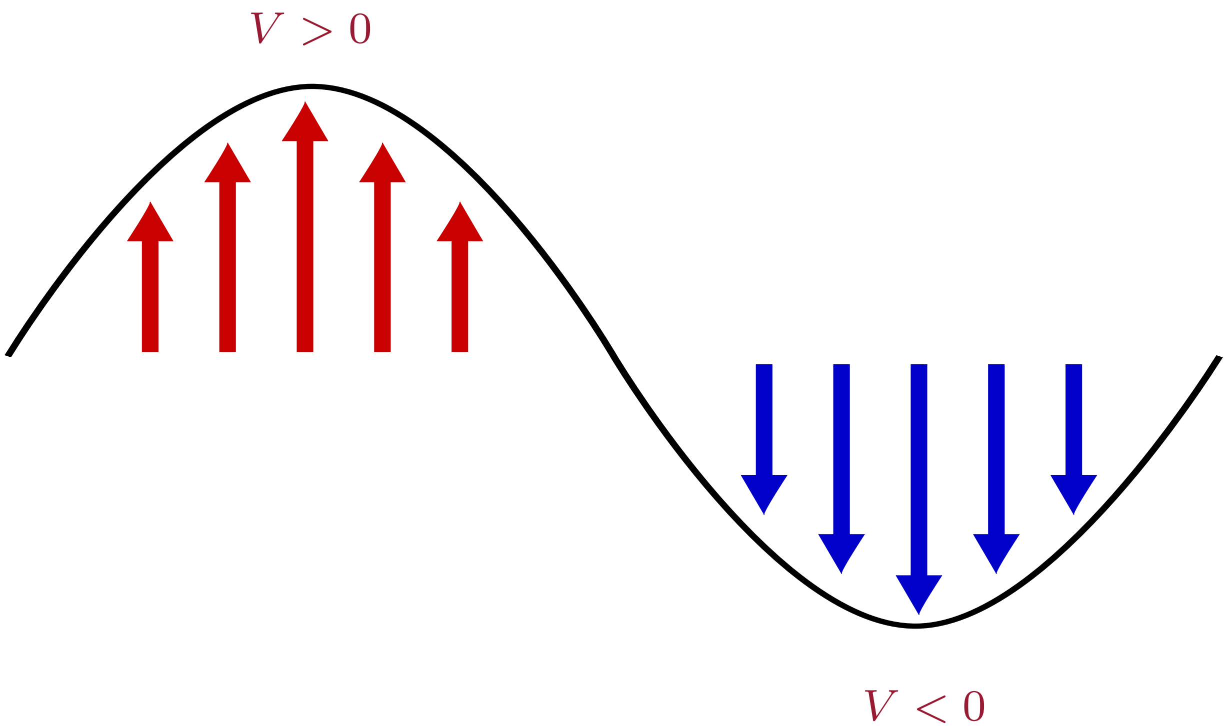

- Barotropic instability occurs in horizontally sheared horizontal flows. It redistributes horizontal momentum.

Barotropic Instability

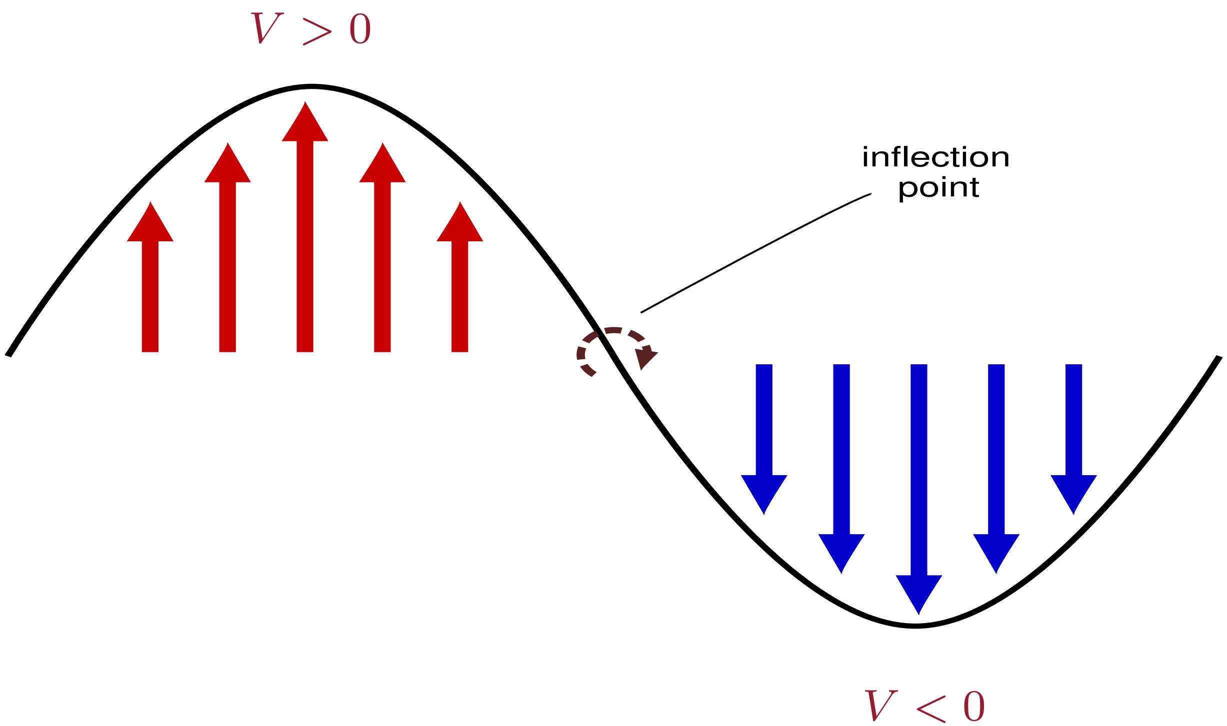

- Barotropic instability occurs in horizontally sheared horizontal flows. It redistributes horizontal momentum.
- A necessary condition for instability is that the flow $V(x)$ have an inflection point (Rayleigh), and furthermore, that it be a maximum of absolute vorticity (Fjortoft).

Barotropic Instability

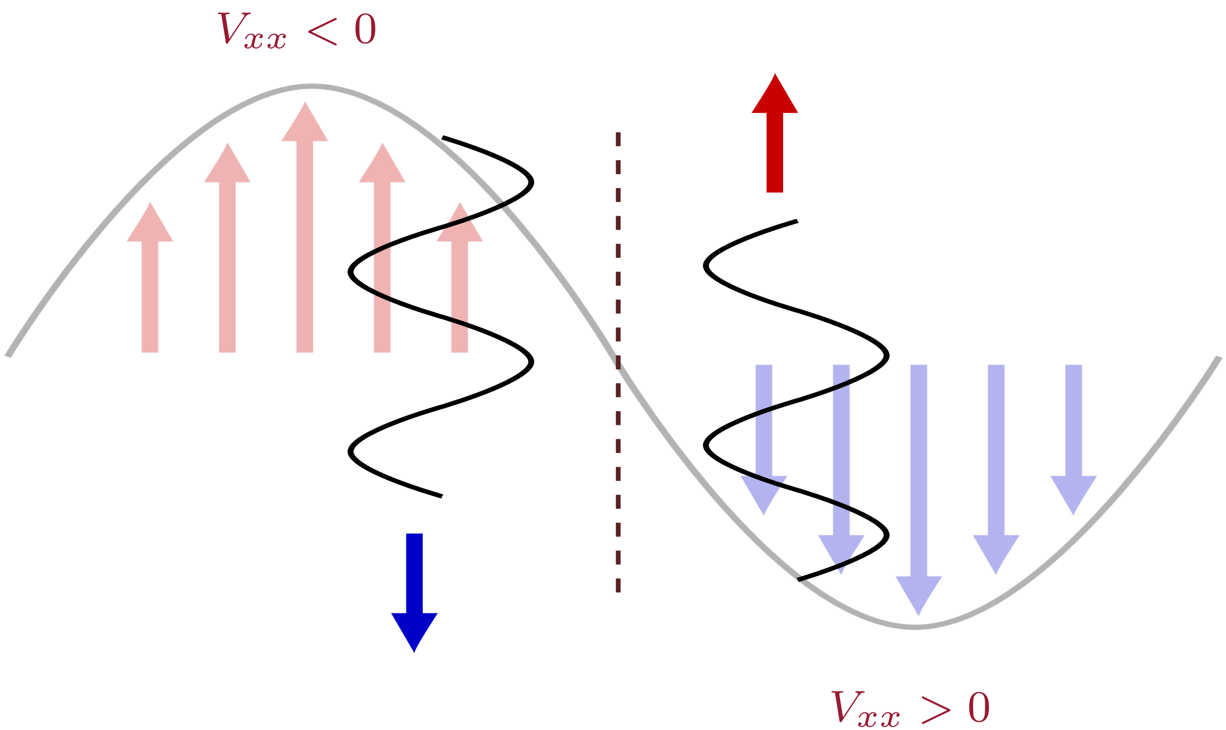

- "Rossby" waves propagate in the positive y direction relative to background flow where $V_{xx} > 0$, and in the negaive y direction where $V_{xx} < 0$.

Approximate dispersion relation: $\dfrac{\omega}{l} \approx V + \dfrac{V_{xx}}{l^2}$

Barotropic Instability

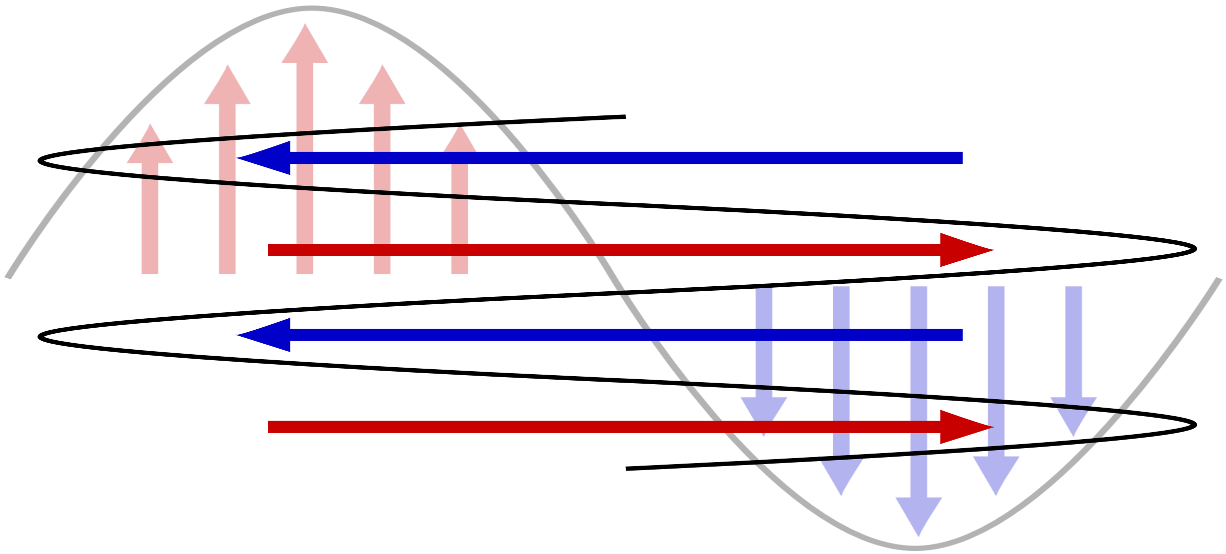

- “Rossby” waves propagate in the positive y direction relative to background flow where $V_{xx} > 0$, and in the negaive y direction where $V_{xx} < 0$.

$$\text{Approximate dispersion relation: } \frac{\omega}{l} \approx V + \frac{V_{xx}}{l^2}$$

- For small enough values of l, waves can phase lock and grow exponentially.

Linear theory in $k \ll -1$ limit

- Scale length and time like $(x, y) = k^{-1}(\xi, \eta)$ and $t = (kV_0)^{-1}\tau$. Basic state wave is:

$$
\begin{aligned}
V &\sim V_0 \exp\left(\frac{-\eta^2}{2k^2}\right)\cos(z)\cos(\xi), \\
U &\sim k^{-1}V_0\left(\frac{\eta}{k}\right)\exp\left(\frac{-\eta^2}{2k^2}\right)\cos(z)\sin(\xi), \\
W &\sim -k^{-2}V_0\left(\frac{\eta}{k}\right)\exp\left(\frac{-\eta^2}{2k^2}\right)\sin(z)\cos(\xi), \\
Z &\sim -kV_0 \exp\left(\frac{-\eta^2}{2k^2}\right)\cos(z)\cos(\xi),
\end{aligned}
$$

Linear theory in $k \ll -1$ limit

- Scale length and time like $(x, y) = k^{-1}(\xi, \eta)$ and $t = (kV_0)^{-1}\tau$. Basic state wave is:

$$
\begin{aligned}
V &\sim V_0 \exp\left(\frac{-\eta^2}{2k^2}\right)\cos(z)\cos(\xi), \\
U &\sim k^{-1}V_0\left(\frac{\eta}{k}\right)\exp\left(\frac{-\eta^2}{2k^2}\right)\cos(z)\sin(\xi), \\
W &\sim -k^{-2}V_0\left(\frac{\eta}{k}\right)\exp\left(\frac{-\eta^2}{2k^2}\right)\sin(z)\cos(\xi), \\
Z &\sim -kV_0\exp\left(\frac{-\eta^2}{2k^2}\right)\cos(z)\cos(\xi),
\end{aligned}
$$

- Perturbation vorticity equation is approximately

$$
\boxed{\tilde{\zeta}'_\tau + \underbrace{V\tilde{\zeta}'_\eta}_{\text{adv. of } \zeta' \text{ by } V} + \underbrace{k^{-1}Z_\xi u'}_{\text{adv. of } Z \text{ by } u'} = \underbrace{\frac{V_0}{k^2}(UZ_\xi + VZ_\eta)}_{\text{self-interaction of wave}}}
$$

Linear theory in $k \ll -1$ limit

- Scale length and time like $(x, y) = k^{-1}(\xi, \eta)$ and $t = (kV_0)^{-1}\tau$. Basic state wave is:

$$
\begin{aligned}
V &\sim V_0 \exp\left(\frac{-\eta^2}{2k^2}\right)\cos(z)\cos(\xi), \\
U &\sim k^{-1}V_0\left(\frac{\eta}{k}\right)\exp\left(\frac{-\eta^2}{2k^2}\right)\cos(z)\sin(\xi), \\
W &\sim -k^{-2}V_0\left(\frac{\eta}{k}\right)\exp\left(\frac{-\eta^2}{2k^2}\right)\sin(z)\cos(\xi), \\
Z &\sim -kV_0\exp\left(\frac{-\eta^2}{2k^2}\right)\cos(z)\cos(\xi),
\end{aligned}
$$

- Perturbation vorticity equation is approximately

$$
\boxed{\tilde{\zeta}'_\tau + \underbrace{V\tilde{\zeta}'_\eta}_{\text{adv. of } \zeta' \text{ by } V} + \underbrace{k^{-1}Z_\xi u'}_{\text{adv. of } Z \text{ by } u'} = \underbrace{\frac{V_0}{k^2}(UZ_\xi + VZ_\eta)}_{\text{self-interaction of wave}}}
$$

- Next order in k^{-1}: time dep. of MRG wave, advection by U, β effect.

Linear theory in $k \ll -1$ limit

- Look for horizontally non-divergent perturbations $u' = -\psi'_\eta$, $v' = \psi'_\xi$. Then

$$\boxed{\nabla^2\psi'_\tau + \cos(z)\exp\left(\frac{-\eta^2}{2k^2}\right)\cos(\xi)\left(\nabla^2\psi'_\eta + \psi'_\eta\right) = \frac{V_0}{k}S[\cos(2\xi), \sin(2\xi), y, z]}$$

- Linear partial differential equation with coefficients periodic in ξ.

Linear theory in $k \ll -1$ limit

- Look for horizontally non-divergent perturbations $u' = -\psi'_\eta$, $v' = \psi'_\xi$. Then

$$\boxed{\nabla^2 \psi'_\tau + \cos(z) \exp\left(\frac{-\eta^2}{2k^2}\right) \cos(\xi) \left(\nabla^2 \psi'_\eta + \psi'_\eta\right) = \frac{V_0}{k} S[\cos(2\xi), \sin(2\xi), y, z]}$$

- Linear partial differential equation with coefficients periodic in ξ.
- Seek solution with periodicity of coefficients (Floquet theorem with exponent $n_0 \equiv 0$).

$$\boxed{\psi'(\xi, \eta, z, t) = \Re\left\{ e^{in_0\xi} \sum_{n=-\infty}^{\infty} \hat{\psi}_n(\eta, t; z) e^{in\xi} \right\}}$$

Linear theory in $k \ll -1$ limit

- Look for horizontally non-divergent perturbations $u' = -\psi'_\eta$, $v' = \psi'_\xi$. Then

$$\boxed{\nabla^2 \psi'_\tau + \cos(z)\exp\left(\frac{-\eta^2}{2k^2}\right)\cos(\xi)\left(\nabla^2\psi'_\eta + \psi'_\eta\right) = \frac{V_0}{k} S[\cos(2\xi), \sin(2\xi), y, z]}$$

- Linear partial differential equation with coefficients periodic in ξ.
- Seek solution with periodicity of coefficients (Floquet theorem with exponent $n_0 \equiv 0$).

$$\boxed{\psi'(\xi, \eta, z, t) = \Re\left\{ e^{in_0\xi} \sum_{n=-\infty}^{\infty} \hat{\psi}_n(\eta, t; z) e^{in\xi} \right\}}$$

- Coefficient proportional to $\cos(\xi)$ couples adjacent terms in the summation.
- $\hat{\psi_0}(\eta, t; z)$ corresponds to the zonally symmetric zonal velocity (the zonal jet).

Linear theory in $k \ll -1$ limit

- Look for horizontally non-divergent perturbations $u' = -\psi'_\eta$, $v' = \psi'_\xi$. Then

$$\boxed{\nabla^2\psi'_\tau + \cos(z)\exp\left(\frac{-\eta^2}{2k^2}\right)\cos(\xi)\left(\nabla^2\psi'_\eta + \psi'_\eta\right) = \frac{V_0}{k}S[\cos(2\xi), \sin(2\xi), y, z]}$$

- Linear partial differential equation with coefficients periodic in ξ.
- Seek solution with periodicity of coefficients (Floquet theorem with exponent $n_0 \equiv 0$).

$$\boxed{\psi'(\xi,\eta,z,t) = \Re\left\{e^{in_0\xi}\sum_{n=-\infty}^{\infty}\hat{\psi}_n(\eta,t;z)e^{in\xi}\right\}}$$

- Coefficient proportional to $\cos(\xi)$ couples adjacent terms in the summation.
- $\psi_0(\hat{\eta}, t; z)$ corresponds to the zonally symmetric zonal velocity (the zonal jet).
- A good approximation is obtained with a three term truncation:

$$\boxed{\psi' \approx \Re\left\{\hat{\psi}_{-1}(\eta,z,t)e^{-i\xi} + \hat{\psi}_0(\eta,z,t) + \hat{\psi}_1(\eta,z,t)e^{i\xi}\right\}}$$

Linear theory in $k \ll -1$ limit

- Substituting the truncated series into the PDE, setting the coefficients of $e^{-i\xi}$, e^0, and $e^{i\xi}$ equal to zero, and discretizing the differential operators in η yields:

$$\boxed{\frac{\partial}{\partial \tau}\boldsymbol{\psi} + \cos(z)\mathbf{A}\boldsymbol{\psi} = \boldsymbol{S}}$$

Linear theory in $k \ll -1$ limit

- Substituting the truncated series into the PDE, setting the coefficients of $e^{-i\xi}$, e^{0}, and $e^{i\xi}$ equal to zero, and discretizing the differential operators in η yields:

$$\boxed{\frac{\partial}{\partial \tau}\boldsymbol{\psi} + \cos(z)\mathbf{A}\boldsymbol{\psi} = \boldsymbol{S}}$$

- where $\boldsymbol{\psi} \equiv [\boldsymbol{\psi}_{-1} \,|\, \boldsymbol{\psi}_{0} \,|\, \boldsymbol{\psi}_{1}]$, and $\mathbf{A}$ is a matrix

Linear theory in $k \ll -1$ limit

- Substituting the truncated series into the PDE, setting the coefficients of $e^{-i\xi}$, e^{0}, and $e^{i\xi}$ equal to zero, and discretizing the differential operators in η yields:

$$\boxed{\frac{\partial}{\partial \tau}\boldsymbol{\psi} + \cos(z)\mathbf{A}\boldsymbol{\psi} = \boldsymbol{S}}$$

- where $\boldsymbol{\psi} \equiv [\boldsymbol{\psi_{-1}} \,|\, \boldsymbol{\psi_0} \,|\, \boldsymbol{\psi_1}]$, and **A** is a matrix
- Unstable modes are eigenvectors of **A** corresponding to eigenvalues with positive real parts.

Linear theory in $k \ll -1$ limit

- Substituting the truncated series into the PDE, setting the coefficients of $e^{-i\xi}$, e^{0}, and $e^{i\xi}$ equal to zero, and discretizing the differential operators in η yields:

$$\boxed{\frac{\partial}{\partial \tau}\boldsymbol{\psi} + \cos(z)\mathbf{A}\boldsymbol{\psi} = \boldsymbol{S}}$$

- where $\boldsymbol{\psi} \equiv [\boldsymbol{\psi_{-1}} \mid \boldsymbol{\psi_0} \mid \boldsymbol{\psi_1}]$, and $\mathbf{A}$ is a matrix
- Unstable modes are eigenvectors of $\mathbf{A}$ corresponding to eigenvalues with positive real parts.

  - Right hand side $\boldsymbol{S}$ acts like an initial seed for the perturbation.
  - Growth rate is proportional to $\cos(z)$.

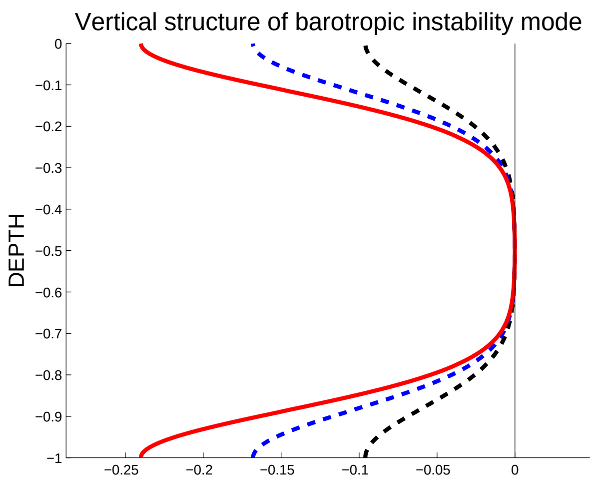

Linear theory in $k \ll -1$ limit

- Most unstable mode for $k = -6.3$:

Zonal mean U

(even and odd modes)

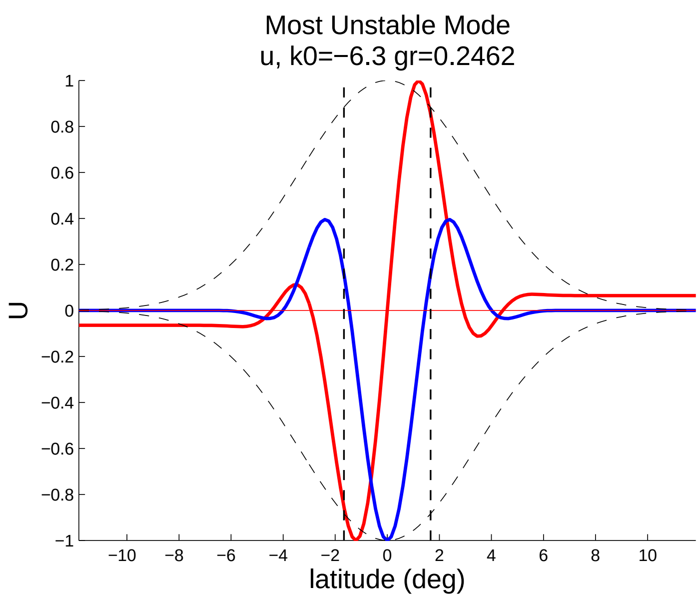

Streamfunction

(of even mode)

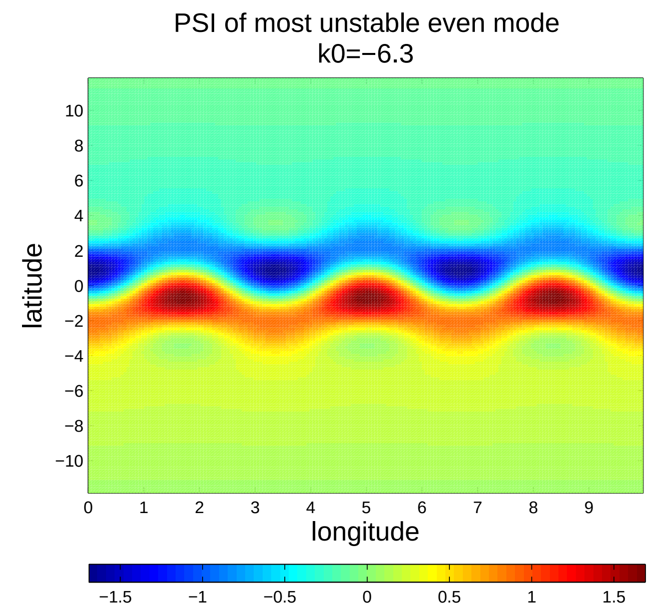

- even and odd modes come in pairs, with odd modes having slightly higher growth rate.

Linear theory in $k \ll -1$ limit

$u_0(y)$ for fastest
growing even eigenmodes

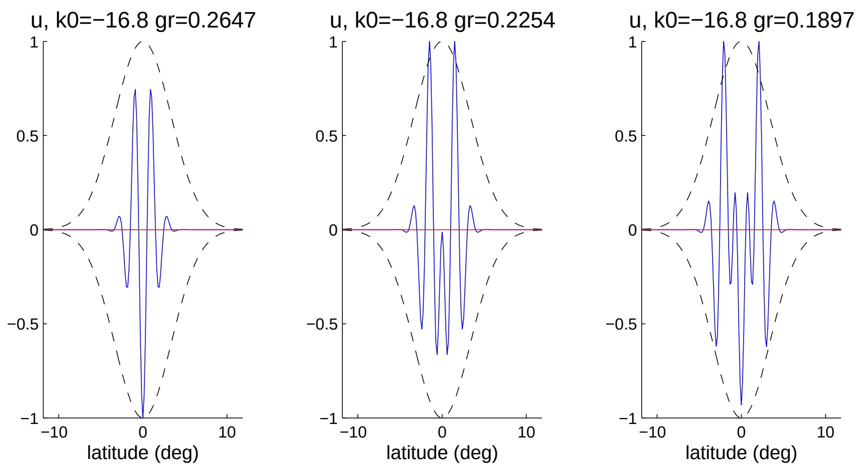

Growth rate vs.
meridional wavenumber

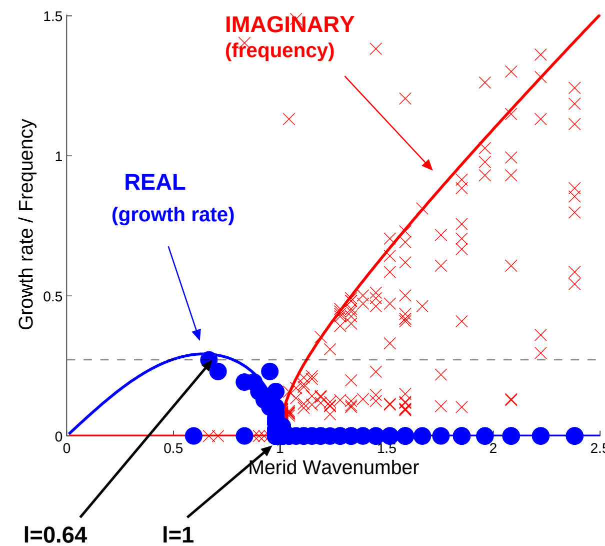

- Jet spacing near equator matches barotropic Rossby wave case (Gill, 1974).
- Jet spacing wider than wavelength of MRG wave $l < 1$.
- Fastest growing jet has width 1.6 times zonal scale of basic state wave.

Comparison with simulations

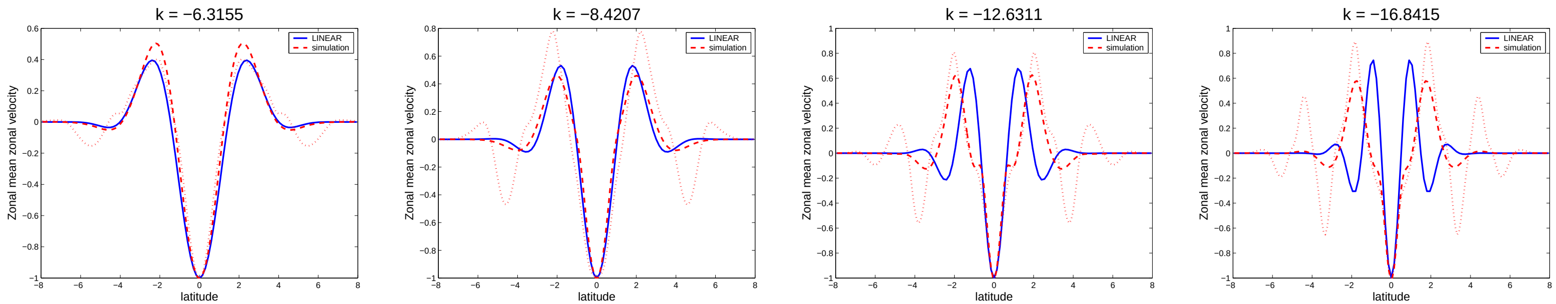

Comparison with simulations

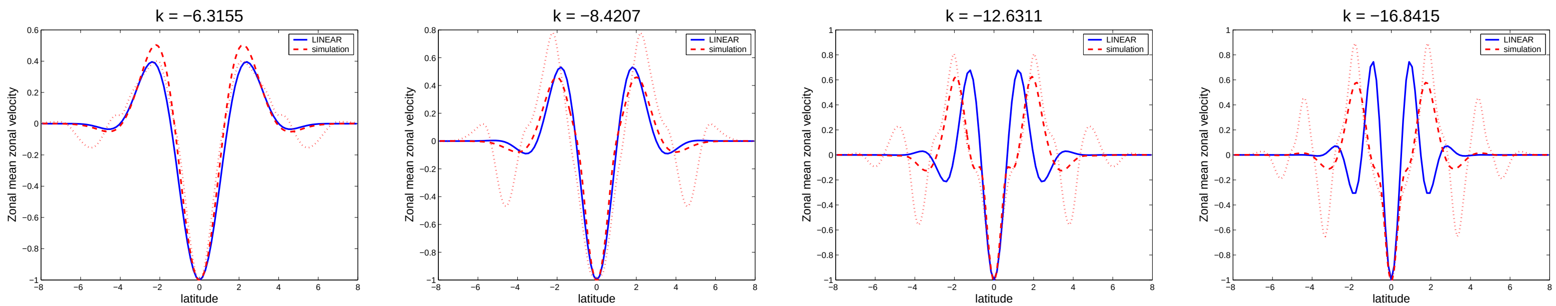

- U even about equator since odd modes inertially unstable

Comparison with simulations

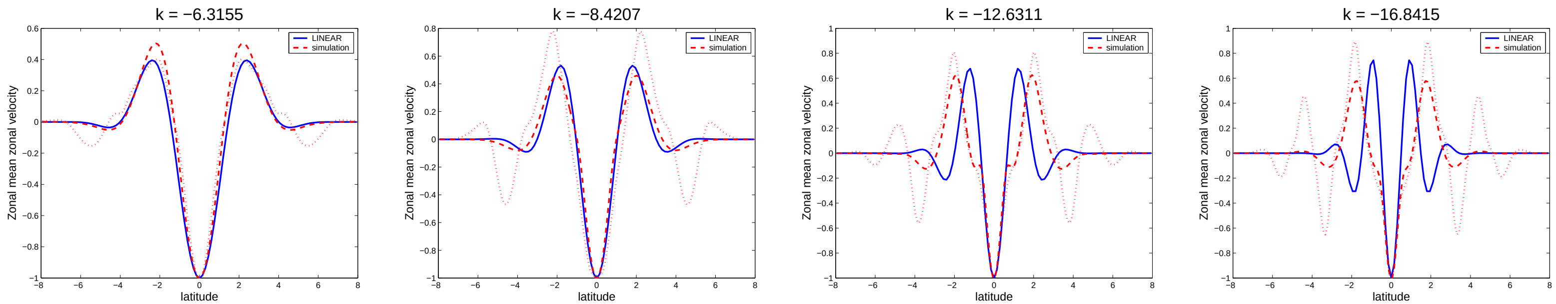

- U even about equator since odd modes inertially unstable
- Equatorial jet always westward. *Probably* due to mixing of planetary angular momentum by zonally short modes (strongest at equator) biasing simulations towards westward flow at equator.

Comparison with simulations

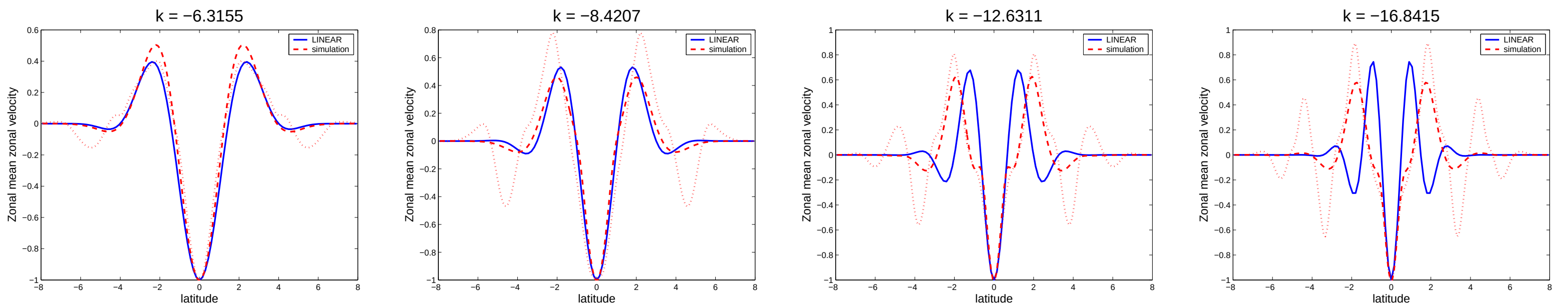

- U even about equator since odd modes inertially unstable
- Equatorial jet always westward. *Probably* due to mixing of planetary angular momentum by zonally short modes (strongest at equator) biasing simulations towards westward flow at equator.
- Extra-equatorial jet positioning poleward of that in most unstable linear mode: barotropic instability?

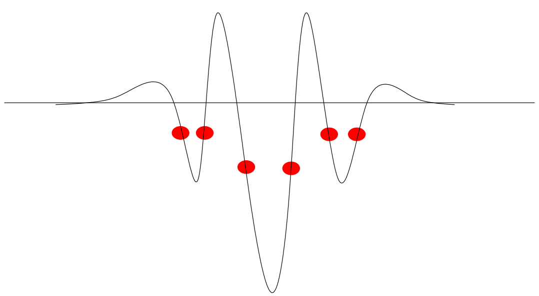

barotropic instability possible when $U_{yy} = \beta$ (does not lead to meridional jets due to Coriolis effect).

Role of inertial instability

- An important mechanism in the development of the zonal jets is inertial instability (Fruman et al., submitted):

Role of inertial instability

- An important mechanism in the development of the zonal jets is inertial instability (Fruman et al., submitted):
  - It forces the meridional phase of the jets to be such that a jet is centred on the equator.

Role of inertial instability

- An important mechanism in the development of the zonal jets is inertial instability (Fruman et al., submitted):
  - It forces the meridional phase of the jets to be such that a jet is centred on the equator.
  - It restricts the maximum amplitude of the equatorial westward jet.

Role of inertial instability

- An important mechanism in the development of the zonal jets is inertial instability (Fruman et al., submitted):
  - It forces the meridional phase of the jets to be such that a jet is centred on the equator.
  - It restricts the maximum amplitude of the equatorial westward jet.
  - It leads to latitudinal homgenization of angular momentum and potential vorticity in the vicinity of the equator.

Role of inertial instability

- An important mechanism in the development of the zonal jets is inertial instability (Fruman et al., submitted):
  - It forces the meridional phase of the jets to be such that a jet is centred on the equator.
  - It restricts the maximum amplitude of the equatorial westward jet.
  - It leads to latitudinal homgenization of angular momentum and potential vorticity in the vicinity of the equator.
  - It leads to vertical mixing of density and tracers in the equatorial track.

Inertial Instability

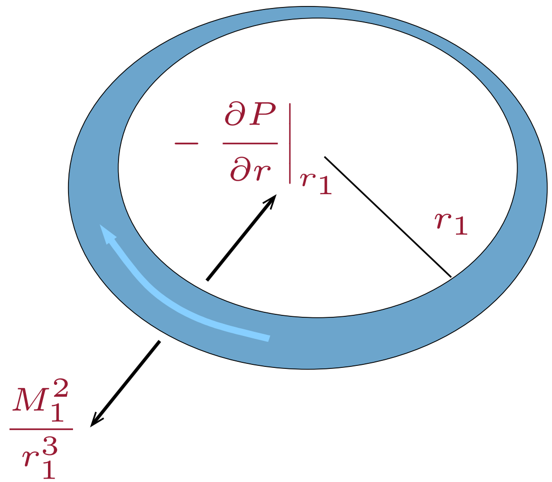

- Balanced centrifugal $\dfrac{M^2}{r^3}$ and pressure gradient $-\dfrac{\partial P}{\partial r}$ forces.

Inertial Instability

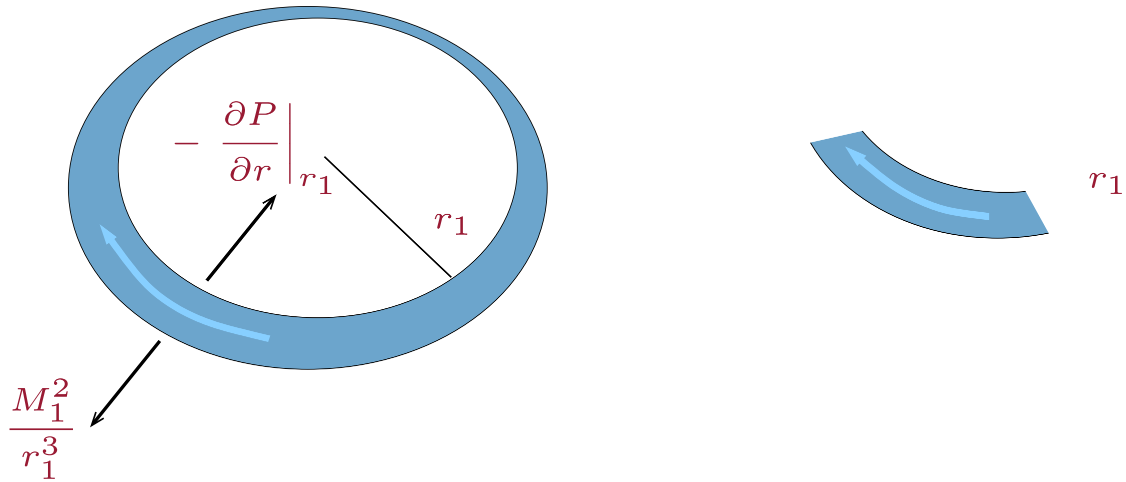

- Balanced centrifugal $\frac{M^2}{r^3}$ and pressure gradient $-\frac{\partial P}{\partial r}$ forces.
- Consider a ring of fluid at r_1

Inertial Instability

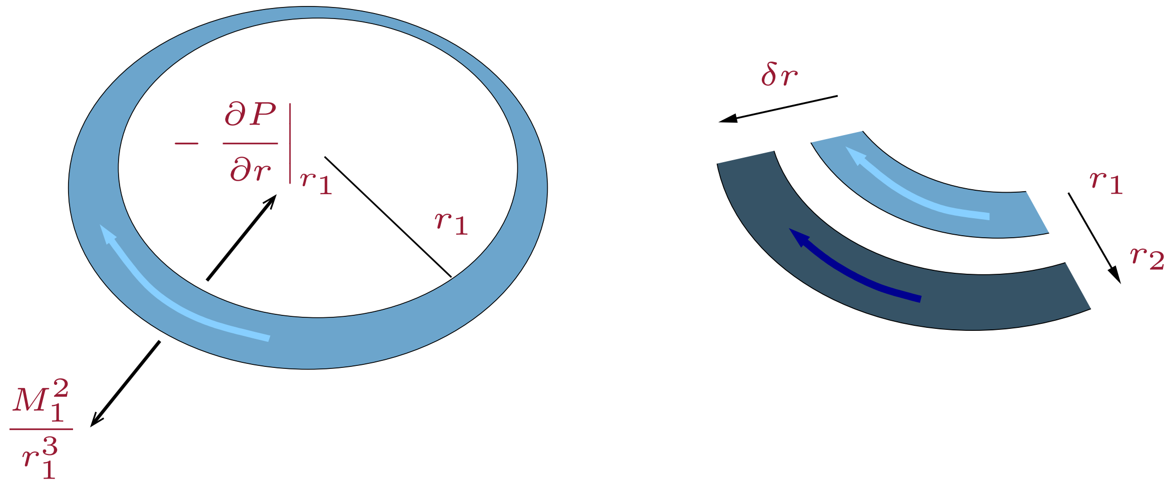

- Balanced centrifugal $\frac{M^2}{r^3}$ and pressure gradient $-\frac{\partial P}{\partial r}$ forces.
- Consider a ring of fluid at r_1 displaced to r_2 conserving its angular momentum without disturbing the pressure field.

Inertial Instability

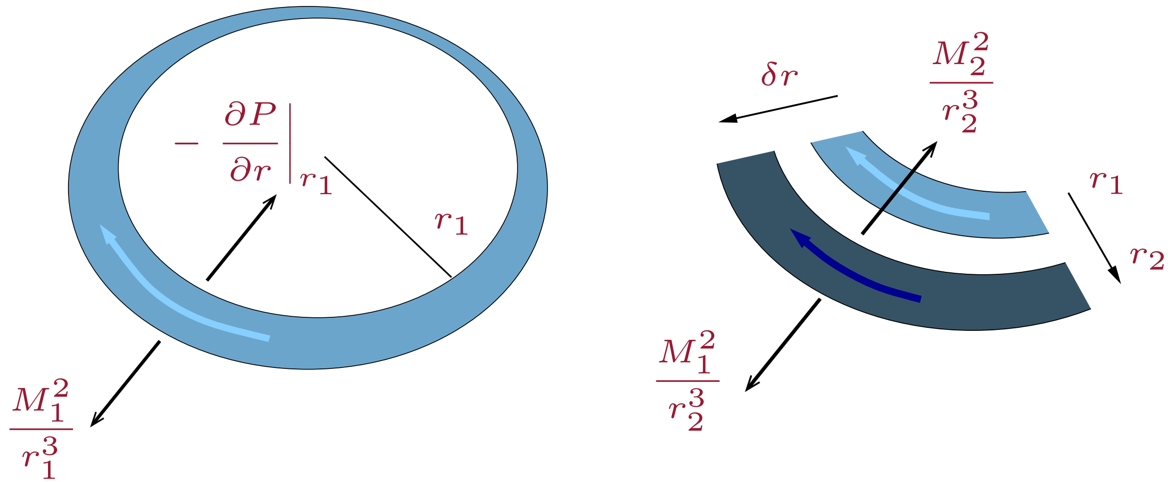

- Balanced centrifugal $\frac{M^2}{r^3}$ and pressure gradient $-\frac{\partial P}{\partial r}$ forces.
- Consider a ring of fluid at r_1 displaced to r_2 conserving its angular momentum without disturbing the pressure field. At its new position, it feels a net radial force

$$\frac{M_1^2}{r_2^3} - \left.\frac{\partial P}{\partial r}\right|_{r_2} = \frac{M_1^2 - M_2^2}{r_2^3} \approx -\frac{1}{r_2^3} \left.\frac{\partial \left(M^2\right)}{\partial r}\right|_{r_2} \delta r$$

Inertial Instability

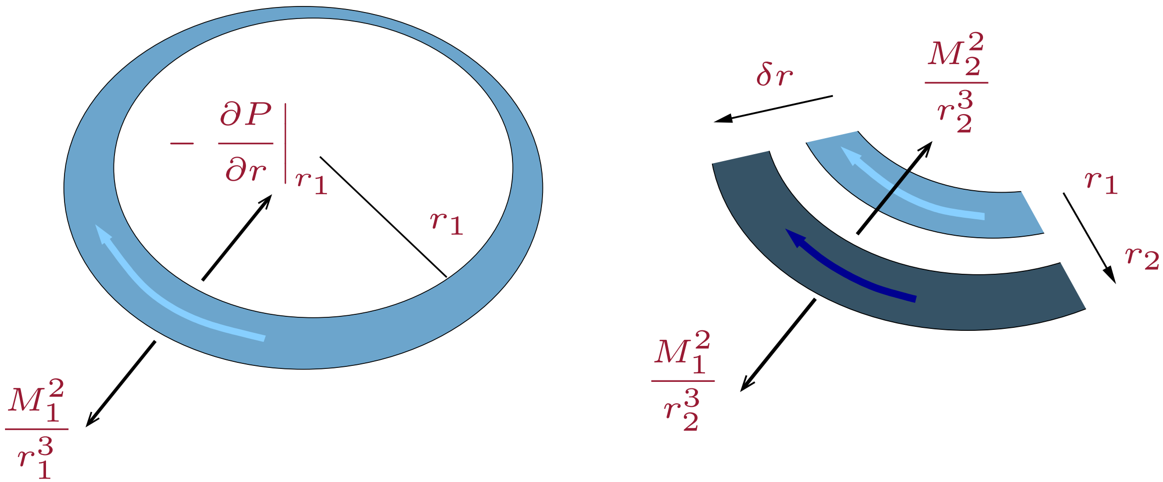

- Balanced centrifugal $\frac{M^2}{r^3}$ and pressure gradient $-\frac{\partial P}{\partial r}$ forces.
- Consider a ring of fluid at r_1 displaced to r_2 conserving its angular momentum without disturbing the pressure field. At its new position, it feels a net radial force

$$\frac{M_1^2}{r_2^3} - \left.\frac{\partial P}{\partial r}\right|_{r_2} = \frac{M_1^2 - M_2^2}{r_2^3} \approx -\frac{1}{r_2^3} \left.\frac{\partial \left(M^2\right)}{\partial r}\right|_{r_2} \delta r$$

$\Longrightarrow$ An axially symmetric flow is inertially stable if $\frac{\partial \left(M^2\right)}{\partial r} > 0$ (Rayleigh, 1917).

Inertial Instability

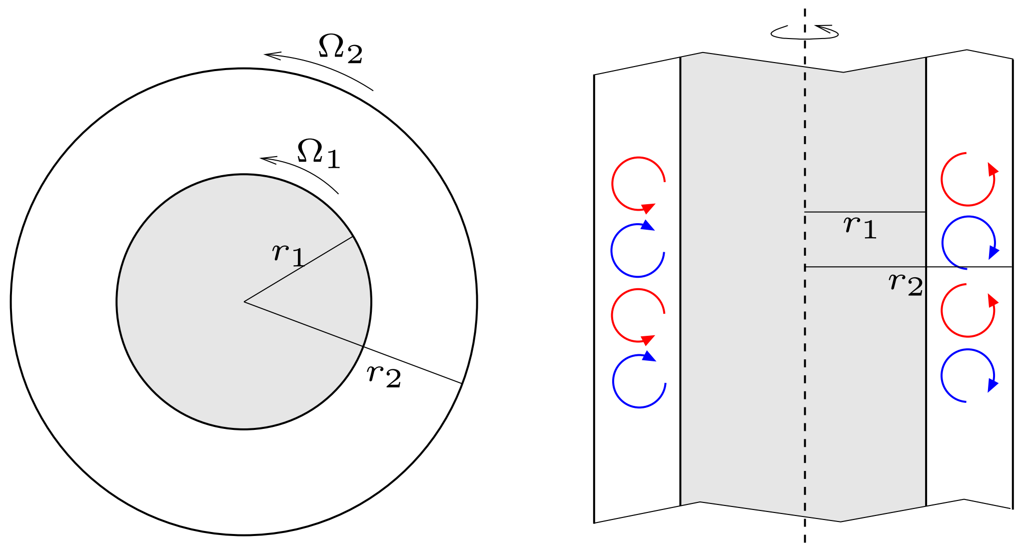

- A famous example of inertial instability is the instability of laminar flow in the Taylor-Couette experiment, when outer cylinder rotates too fast relative to inner cylinder (Taylor (1923)).

Inertial Instability

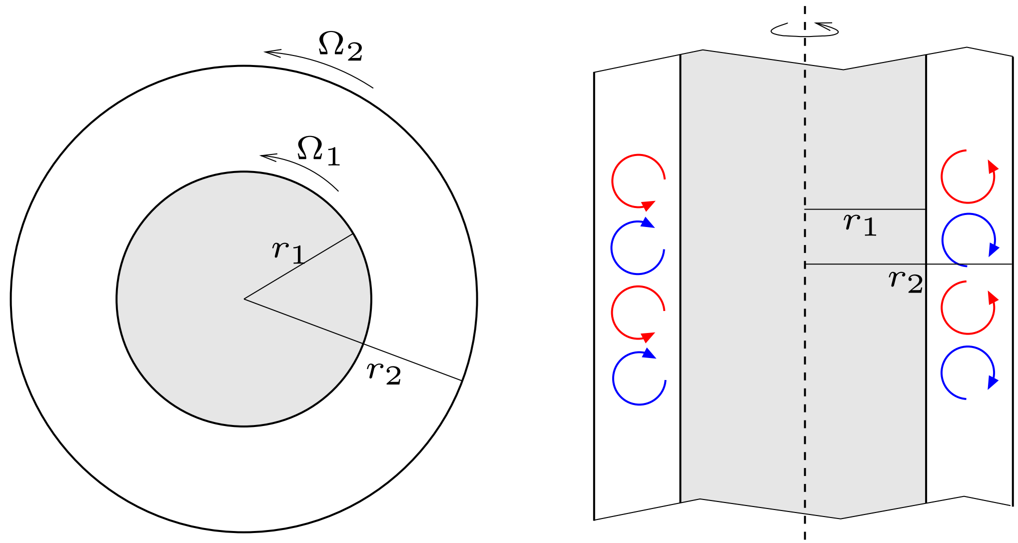

- A famous example of inertial instability is the instability of laminar flow in the Taylor-Couette experiment, when outer cylinder rotates too fast relative to inner cylinder (Taylor (1923)).
- First bifurcation leads to Taylor vortices in the radial-vertical plane.

Inertial Instability

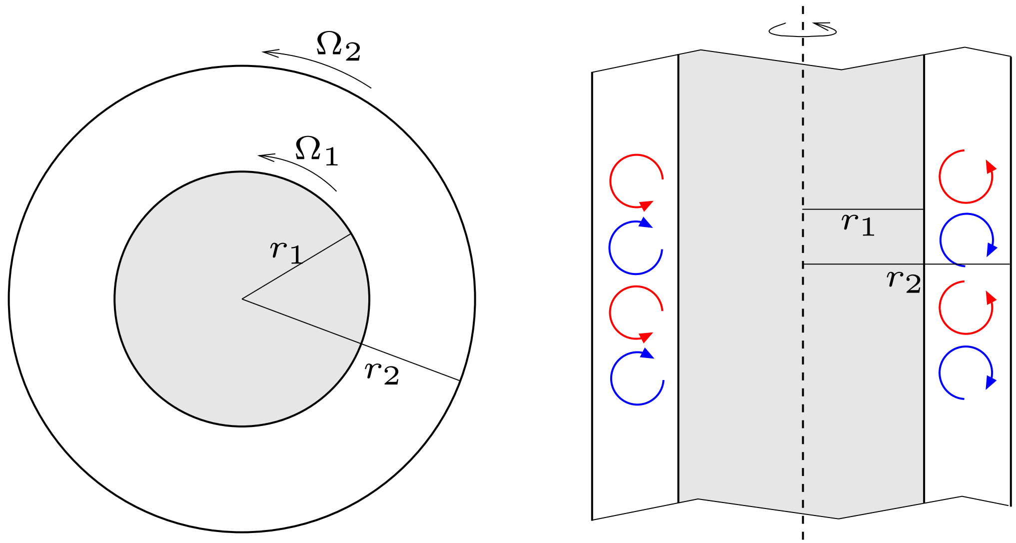

- A famous example of inertial instability is the instability of laminar flow in the Taylor-Couette experiment, when outer cylinder rotates too fast relative to inner cylinder (Taylor (1923)).
- First bifurcation leads to Taylor vortices in the radial-vertical plane.
- For inertial stability on the earth, maximum angular momentum must be at the equator.
- Combined with effects of stratification, the condition for stability is that Potential Vorticity have the sign of latitude ("symmetric stability").

Inertial Instability

- For stability, maximum angular momentum $M \approx U - \frac{1}{2}\beta y^2$ must be at the equator:

Equatorial shear inertial instability

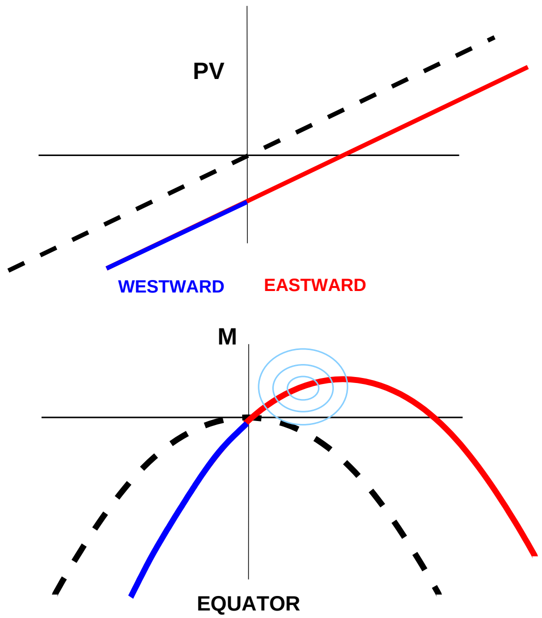

(Dunkerton, 1981)

$U = \lambda y$, unstable for all $\lambda \neq 0$

Adjustment mixes in latitude and depth.

"Curvature" inertial instability

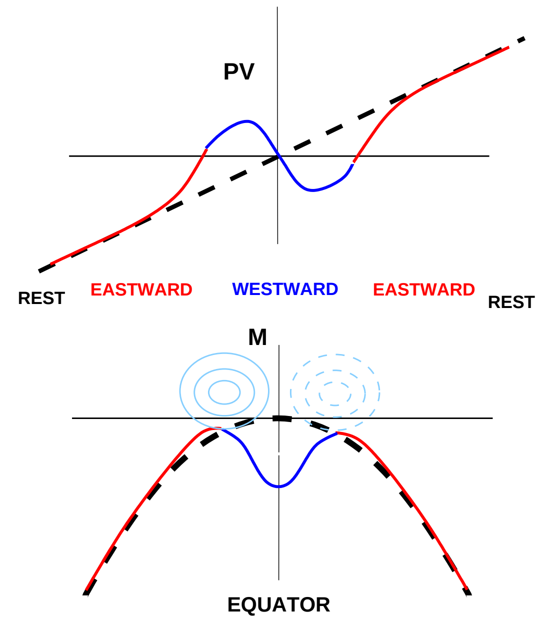

$U = (-U_{00} + \frac{1}{2}by^2)e^{-\frac{1}{2}y^2}$, unstable for $b > \beta$

Inertial Instability

- For stability, maximum angular momentum $M \approx U - \frac{1}{2}\beta y^2$ must be at the equator:

Equatorial shear
inertial instability

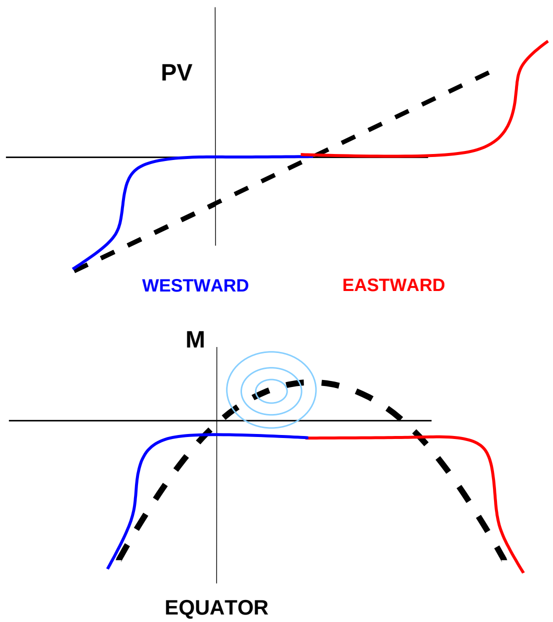

“Curvature”
inertial instability

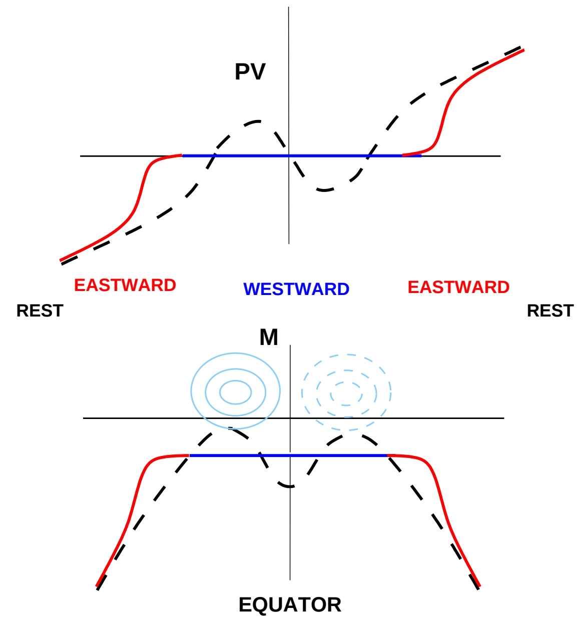

- inertial adjustment takes place over wider latitude interval than covered by initial instability (Hua et al., 1997, Griffiths, 2003).
- Results in wide area of zero PV.

Inertial instability in simulations

- Evidence of inertial instability in the simulations:

Absolute vorticity vs. latitude

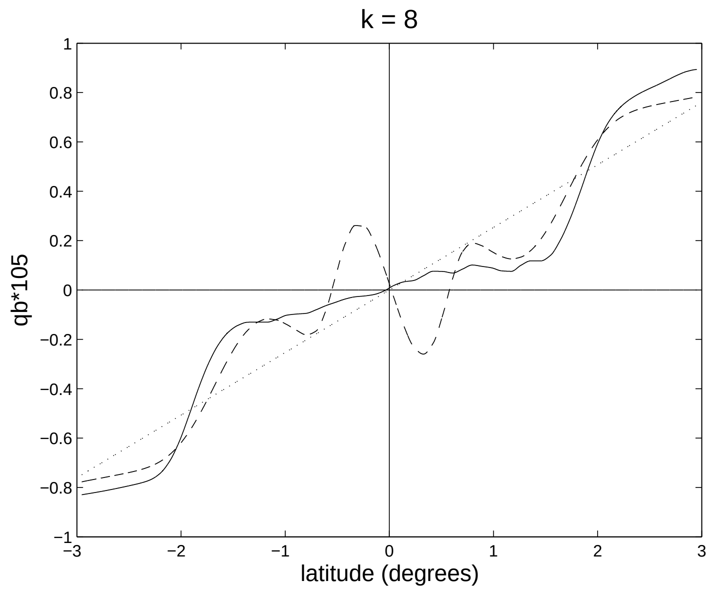

Jet amplitude and anomalous PV

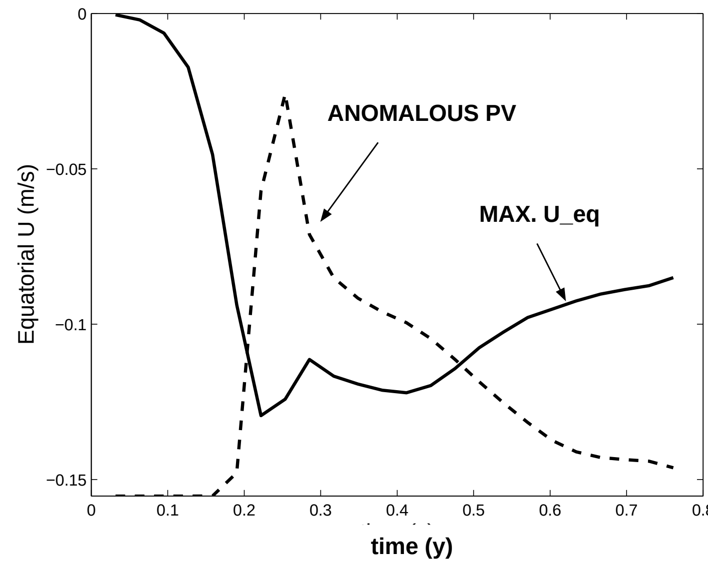

- Also, energy increase in zonally symmetric components of v and w fields.

Baroclinic equatorial deep jets

- If the instability is barotropic, why are the jets seen in the observations and in basin simulations (d’Orgeville et al., 2007) alternating in sign with depth?

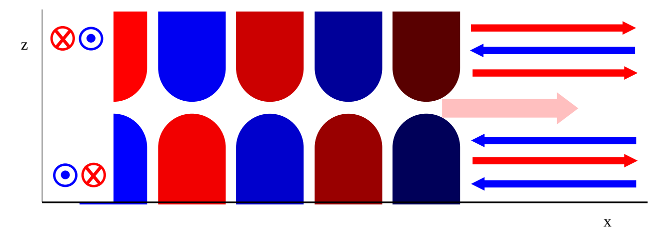

Baroclinic equatorial deep jets

- If the instability is barotropic, why are the jets seen in the observations and in basin simulations (d'Orgeville et al., 2007) alternating in sign with depth?

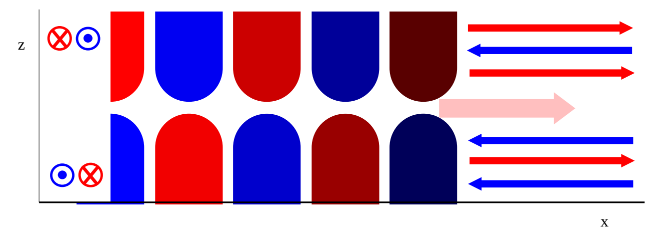

- Hua et al., 2008:
  - Since the destabilization is taking place mostly in the western edge of the basin, what is observed in the remainder of the basin is the projection of the jets pattern onto low-frequency, long zonal wavelength waves with eastward group velocities.
  - The only such wave is the equatorial Kelvin wave, which has

$$u(y,z) \propto \cos(mz)\exp\left[-\left(\frac{\beta m}{2NH}\right)y^2\right]$$

  - The vertical mode m of the observed jets corresponds to the vertical mode of the Kelvin wave with meridional width $\sqrt{NH/\beta m}$ comparable to the width of the most unstable barotropic jet mode, namely $m \propto k^2 \propto T^2$.

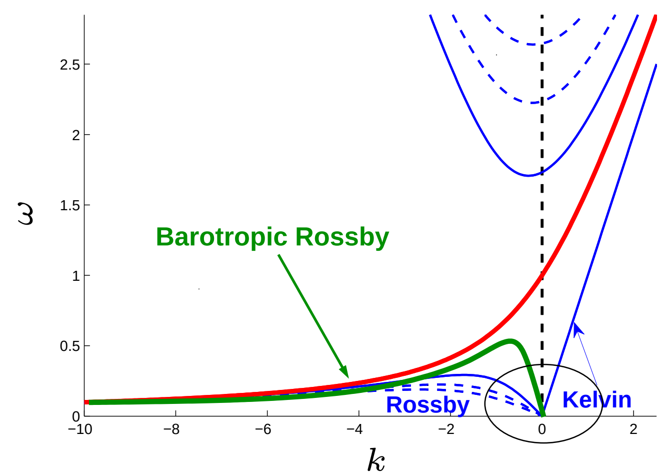

Layering, zonal jets, and inertial instability

- Inertial instability is also important for mixing of density and tracers in the equatorial track, a potentially important element in balancing the global mass circulation.

Layering, zonal jets, and inertial instability

- Inertial instability is also important for mixing of density and tracers in the equatorial track, a potentially important element in balancing the global mass circulation.

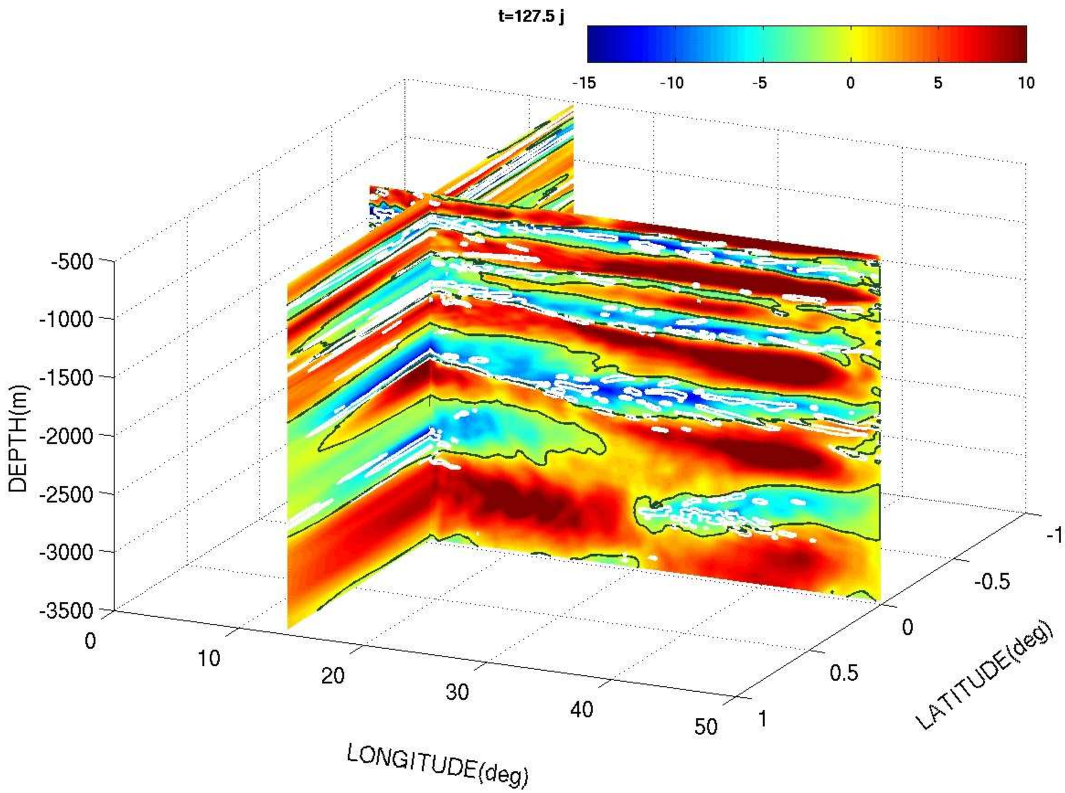

(Ménesguen et al., submitted)

- Regions of vertical mixing are concentrated in westward jets, and are strongly correlated with the criterion for marginal inertial instability.

Summary

- Zonal jets in the equatorial oceans can be generated in high resolution numerical simulations by the barotropic instability of low frequency equatorial waves. (d'Orgeville et al., 2007)

Summary

- Zonal jets in the equatorial oceans can be generated in high resolution numerical simulations by the barotropic instability of low frequency equatorial waves. (d'Orgeville et al., 2007)
- A truncated Floquet series solution to the linearized vorticity equation for barotropic perturbations predicts jet widths and number from simulations.

Summary

- Zonal jets in the equatorial oceans can be generated in high resolution numerical simulations by the barotropic instability of low frequency equatorial waves. (d'Orgeville et al., 2007)
- A truncated Floquet series solution to the linearized vorticity equation for barotropic perturbations predicts jet widths and number from simulations.
- Jet positioning and equilibration amplitude is explained in terms of inertial stability. (Fruman et al., submitted)

Summary

- Zonal jets in the equatorial oceans can be generated in high resolution numerical simulations by the barotropic instability of low frequency equatorial waves. (d'Orgeville et al., 2007)
- A truncated Floquet series solution to the linearized vorticity equation for barotropic perturbations predicts jet widths and number from simulations.
- Jet positioning and equilibration amplitude is explained in terms of inertial stability. (Fruman et al., submitted)
- Baroclinic Equatorial Deep Jets predominate in basin simulations because they correspond to Kelvin waves, which have eastward group velocities. (Hua et al., 2008)

Summary

- Zonal jets in the equatorial oceans can be generated in high resolution numerical simulations by the barotropic instability of low frequency equatorial waves. (d'Orgeville et al., 2007)
- A truncated Floquet series solution to the linearized vorticity equation for barotropic perturbations predicts jet widths and number from simulations.
- Jet positioning and equilibration amplitude is explained in terms of inertial stability. (Fruman et al., submitted)
- Baroclinic Equatorial Deep Jets predominate in basin simulations because they correspond to Kelvin waves, which have eastward group velocities. (Hua et al., 2008)
- Inertial instability leads to vertical mixing of density and tracers in equatorial track. (Ménesguen et al., submitted)

Continuing Work

- Very short wavelength waves lead to local super-rotation. Application to planetary atmospheres?
- Baroclinic effects of depth-dependent triggering of inertial instability.
  - The effect of the non-traditional Coriolis force? Simulations show strong vertical symmetry breaking. Evidence of global conservation of angular momentum for wave momentum flux?